Impacts of land use–based carbon emission pattern on surface temperature dynamics: Experience from the urban and suburban areas of Khulna, Bangladesh

Article *in* Remote Sensing Applications Society and Environment · April 2021

DOI: 10.1016/j.rsase.2021.100508

CITATIONS
30

READS
204

3 authors:

Md. Abdul Fattah
Florida State University
57 PUBLICATIONS **747** CITATIONS
SEE PROFILE

Syed Riad Morshed
Sheltech Consultants (Pvt.) Ltd
37 PUBLICATIONS **353** CITATIONS
SEE PROFILE

Syed Yad Morshed
RMG Sustainability Council (RSC)
7 PUBLICATIONS **131** CITATIONS
SEE PROFILE

Remote Sensing Applications: Society and Environment 22 (2021) 100508

Contents lists available at ScienceDirect

Remote Sensing Applications: Society and Environment

journal homepage: http://www.elsevier.com/locate/rsase

Impacts of land use-based carbon emission pattern on surface temperature dynamics: Experience from the urban and suburban areas of Khulna, Bangladesh

Md. Abdul Fattah [a,*], Syed Riad Morshed [a], Syed Yad Morshed [b]

[a] Department of Urban and Regional Planning, Khulna University of Engineering and Technology, Khulna, Bangladesh
[b] Department of Civil Engineering, Khulna University of Engineering and Technology, Khulna, Bangladesh

ARTICLE INFO

Keywords:
Khulna
Land surface temperature
Land specific carbon emissions

ABSTRACT

The human-oriented urban development process significantly affects the thermal environment of cities and surrounding areas by transforming the eco-friendly land use and land cover (LULC) and increasing carbon emission. The impact of such effects is relatively higher in developing countries like Bangladesh, due to unplanned urbanization. The study aimed to examine the influences of land-specific carbon emissions (LCEs) on land surface temperature (LST) dynamics in the urban and suburban areas of Khulna city during 1998–2018. Landsat images of the year 1998, 2008, and 2018 were used to estimate LULC, LST, and LCEs change over the last two decades and documented the LCEs and LST change pattern in both urban and suburban areas. The association between LCEs and LST was examined through linear regression in the GIS environment. The experimental result indicates that (i) carbon emission sources in urban areas and carbon sinks in suburban areas have increased (ii) lowest LST was documented in carbon sinks and the highest LST in the carbon sources (iii) the correlation coefficients were 0.82651, 0.83771 and 0.89216 which indicates the strong significant impacts of LCEs on the increase of LST and become higher and higher from 1998 to 2018, (iv) LST responded highly to the increase of LCEs in the urban areas than in the suburban areas and increased LST of urban areas by 5.54 °C. The study signifies the necessity of taking proper policies and strategies immediately for sustainable urban development and the habitable sound environment.

1. Introduction

Urbanization and industrialization have been continuously influencing the rapid transformation of eco-friendly land use and land cover (LULC), change of biological systems, and rise of greenhouse gas (GHG) (Cui et al., 2018). GHG emissions are now a major concern regionally and globally because of numerous changes in the environment (Mohajan, 2014). Spontaneous expansion of urban area and increase of urban activities has resulted in the speedy increase of carbon emissions and environmental degradation. The sources and sinks of carbon from LULC have a significant influence on the global carbon budget (Minnen et al., 2009). The rise of GHG emissions, directly and indirectly, increasing global temperature. LULC contributed about 33% of total emissions over the last 150 years to anthropogenic carbon emissions; 20% in 1980 and 1990; and 12.5% from 1990 to 2010 (Houghton et al., 2012). The spatial carbon concentrations have crossed the limit of 350 ppm and increased from the CO_2 equivalent of 280 ppm–450 ppm (Stern, 2014). According to IPCC, the global temperature will rise by 1.1 °C–6.4 °C in this century and Bangladesh by 1–1.5 °C by 2050 (Jain et al., 2015). Carbon emissions (CEs) and their adverse impacts on surface temperature, global temperature, and the environment are increasing rapidly and have been causing serious health problems to the living being (Lai et al., 2016). That's why researchers have been highly motivated by this phenomenon to mitigate such problems.

Soil is known as Earth's largest source of carbon in terrestrial systems and holds a significant role in the global carbon cycle (Prabha et al., 2019). Human activities such as urbanization, fossil fuel burning, LULC change, etc. have been increasing carbon emission (Quéré et al., 2009). Forest land, vegetation, waterbody, vacant LULC types have the potential to absorb GHG as well as reduce CEs and have a significant share of

* Corresponding author. Khulna University of Engineering and Technology, Khulna, Bangladesh.
E-mail addresses: mafattah.kuet@gmail.com, mafattah.kuet@gmail.com (Md.A. Fattah), riad.kuet.urp16@gmail.com (S.R. Morshed), yadmorshed@gmail.com (S.Y. Morshed).

https://doi.org/10.1016/j.rsase.2021.100508
Received 23 October 2020; Received in revised form 13 March 2021; Accepted 29 March 2021

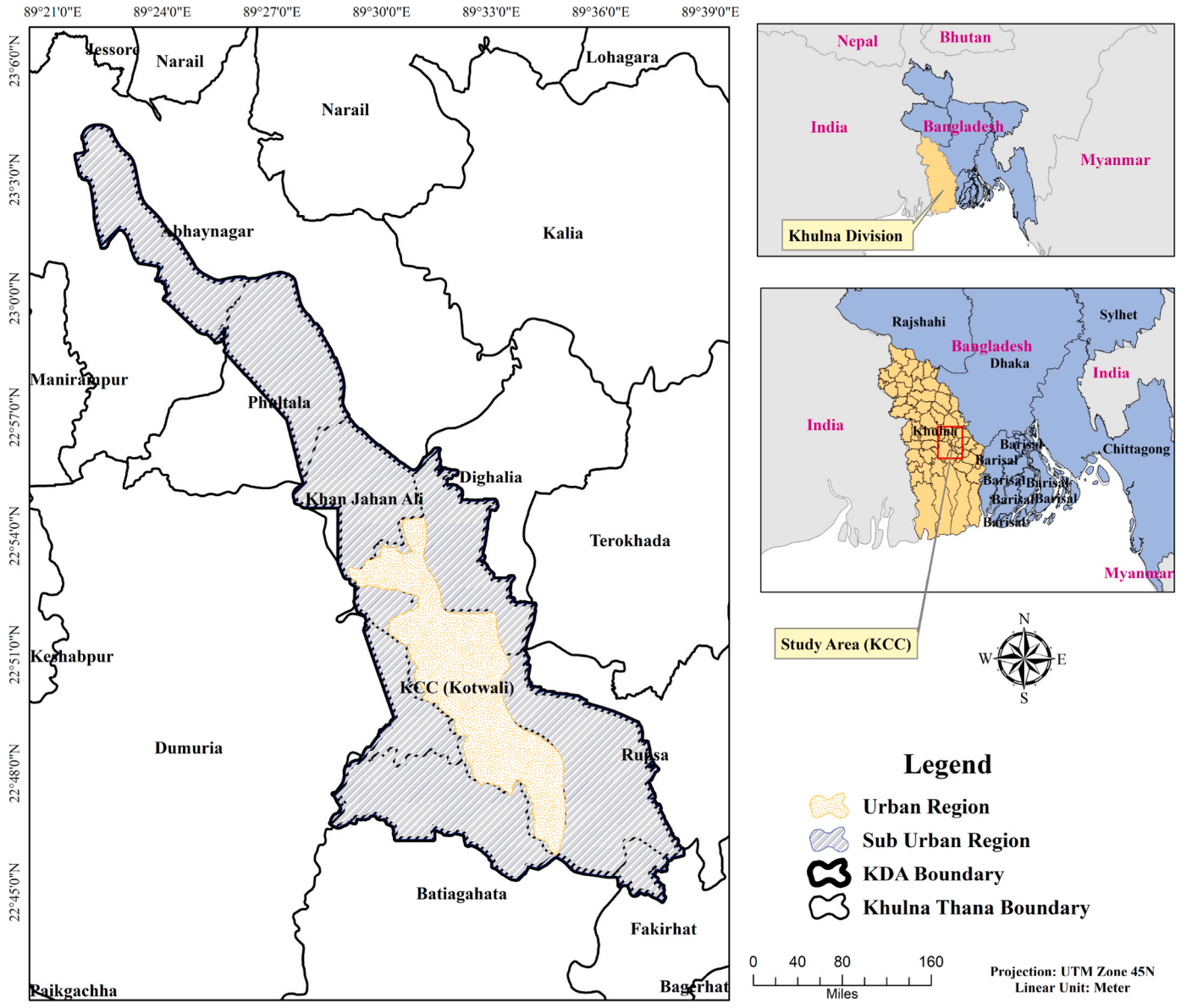

Fig. 1. Study area map showing the urban and suburban unit.

ecosystem services. Changes in LULC type can contribute significantly to global climate change (Fattah et al., 2021). Land cover types such as vegetation and soils naturally act as a sink of carbon and store carbon dioxide absorbed by photosynthesis (Houghton et al., 2012). The built-up area works as one of the main carbon emission sources in an urban area. Declination and transformation of landforms that can absorb carbon, GHG like CO_2, NO_2, CH_4, SO_2, etc. increasing in the atmosphere which contributes to global warming (Maheshwari et al., 2018; Florides and Christodoulides, 2009). Due to urban expansion, the CEs and the impact of CEs are increasing in cities as well as suburban areas. Researchers, engineers, and environmentalists blamed anthropogenic CO_2 emissions for the unprecedented increase of earth surface temperature and global warming (Fang et al., 2011). Thus, LULC change and CEs directly have impacts on land surface temperature (LST) dynamics. Scientists fear that a significant rise of LST will cause a serious adverse effect on the natural environment.

Due to population growth, living, modernization, and better jobs, and lifestyle people are stirring towards the city. Which is promoting urbanization and industrialization and has been creating inverse effects on the LULC of the urban areas. Minnen et al. (2009), Houghton et al. (2012), Baccini et al. (2012) have shown that land cover change has more influence on CEs than burning fossil fuel. The net CEs due to LULC change estimated 12.5% of the 1990 to 2010 anthropogenic CEs and 33% of total emissions over the last 150 years (Baccini et al., 2012). The net CEs from LULC change has been documented mostly in the carbon budget and accounted for 1.4 (range: 0.4 to 2.3) $PgCyr^{-1}$, 1.6 (0.5–2.7) $PgCyr^{-1}$, and 1.1 $\pm$ 0.7 $PgCyr^{-1}$ during the 1980s, 1990s and between 2000 and 2009 respectively (Friedlingstein et al., 2010). According to the IPCC report, the global average temperatures increasing rate was highest in the last century because of the intensification in anthropogenic GHG emission that contributed to global surface warming (Fang et al., 2011).

Cities with a large population and substantial economic activity have high LST, induced by urban and anthropogenic heating sources, GHG emission, and eco-friendly land cover type declination (Gazi et al., 2020). Most of the areas of Bangladesh are experiencing rapid urbanization and ecosystem degradation (Islam and Ma, 2018). BBS (2011) showed that, as a result of urban expansion, roads, and infrastructural development, the country is losing 809 km^2 of cropland each year. Since declination of ecofriendly LULC type has severe destructive impacts of

GHG emission as well as global warming (Fattah et al., 2021), therefore, identification and monitoring of land-use-based carbon emission and LST changing pattern of fast-growing city Khulna is very much crucial. Moreover, very little researches have been done regarding this aspect. Most of the recent studies have focused on the CE characteristics of economically developed regions (Chuai et al., 2014; Cui et al., 2018) but insufficient studies have been done for developing countries like Bangladesh. Furthermore, the LCEs pattern in urban and suburban areas and their influences on LST are not detailed in the previous studies. Besides, for a sustainable green environment developing countries should give more focus on GHG emission pattern, change, and their impact on the environment and should include this in land use planning.

This study documented the influence of LULC on carbon emission dynamics and the impact of land use-based carbon emission on the LST dynamics and detailed the nexus between LCEs and LST of urban, and suburban areas using the remote-sensing application. Duguma et al. (2019); Lin et al. (2018) and Don et al. (2011) showed the impact of LULC change on CEs change, the impact of carbon emission on the environment in the literature (Florides and Christodoulides, 2009; Maheshwari et al., 2018; Sahana et al., 2016; Jain et al., 2015). Jeevalakshmi et al. (2017); Ning et al. (2018); Peng et al. (2017); Guha et al. (2018); Zullo et al. (2019) have shown the impact of LULC on LST in the contest of different locations around the world. Several studies have also shown the association between LULC and LST in the context of different cities in Bangladesh. Such as (Ahmed, 2011; Parvin and Abudu, 2017; Raja and Neema, 2013; Ahmed et al., 2013) on Dhaka (Gazi et al., 2020; Islam and Ma, 2018; Maksudurrahman, 2018), on Chittagong (Kafy et al., 2019; Kafy et al., 2020) on Rajshahi. These studies were conducted for dense urban areas, while tropical urban and suburban areas have been less studied. This study filled all these gaps and illustrated the LULC, LCEs and LST changing pattern, identified the impact of LCEs pattern on LST of urban and suburban areas.

2. Methods and materials

2.1. Study region

Bangladesh is a developing country located in the South Asia region, aimed to achieve the title of developed country by 2041. This is a riverine country and has a climate of sub-tropical monsoon, characterized by wide seasonal variations in humidity, rainfall, and temperatures. Three distinct seasons namely, winter (October–March), humid summer (March–June), and the rainy season (June–October) are seen with the maximum average temperature range 30 °C and 40 °C during summer (Mondal et al., 2017). Khulna is the largest district of the Khulna division of Bangladesh, and Khulna City Corporation (KCC) is the administrative center and the urban area of Khulna district. In this study, Khulna Development Authority (KDA) area is considered as the study unit (Fig. 1). At the center of the KDA area is KCC which is a fast-growing urban area of Bangladesh and the rest portion is the suburban area (Ahmed, 2011). Due to many natural and manmade reasons, the environment of this region is degrading day by day. The suburban areas of Khulna were famous for Jute cultivation and over the past two decades, shrimp cultivation has increased here (Morshed et al., 2020b), on the other hand, industrialization and infrastructural development has increased in the urban area (Fattah et al., 2021). The rationale behind selecting this area as the study region that urbanization, natural calamities, and manmade hazards have adversely affected the environment, natural ecosystem, especially over the past few decades (Haque et al., 2014). The total area of KDA area is 233.66 sq. km where the urban area (KCC) is 45.154 sq. km and the suburban area is 188.506 sq. km. The average temperature of the Khulna is 26.37 °C that has been increasing with a rate of 0.005 °C/year over the past few decades and the precipitation is 1630 mm. The average altitude of the study unit is 1.8 m above mean sea level. Tropical monsoon climate prevails in this area with cool winters and humid and hot summers (Mondal et al., 2017).

Table 1
Details of the used Landsat satellite images.

Satellite/ Sensor	Pixel Size	Spectral Resolution	Resolution	Path/ Row	Date
LANDSAT 5		Multispectral (6 Bands)			April 06, 1998
LANDSAT 5	30	Multispectral (6 Bands)	30 m	137/44	April 17, 2008
LANDSAT 8		Multispectral (11 Bands)			April 11, 2018

2.2. Dataset preparation

We have collected three Multispectral Landsat satellite images from USGS for the period of 10 years from 1998 to 2018 to measure the LULC, LCEs and LST in the study region. These satellite images were of 30m resolutions (30 × 30 pixels) and were collected for April to avoid the impacts of seasonal variations. Though cloud cover for all the three images was set as less than 10%, it was close to zero. The information about the Landsat scenes is presented in Table 1. The atmospheric data were collected from Bangladesh Meteorological Department (BMD) to verify if there was adverse weather that could affect the LST result.

2.3. LULC classification and mapping

LULC classification is one of the key remote sensing applications to identify the characteristics of land use by using multispectral satellite imagery. Remotely sensed images are classified by supervised and unsupervised methods (Kafy et al., 2019). In this study, we have applied the maximum likelihood classifier (MLC) method, which is mostly used for image classification due to its availability, simplicity and could produce LULC maps with high classification accuracies (Li et al., 2014). Before image classification, the preparation of satellite images is essential to avoid these errors and to create a closer link between the data obtained and biophysical characteristics on the ground (Alawamy et al., 2020). Radiometric, atmospheric and geometric corrections have been done to fill the image gap and enhancement. In this study, the generation of composite band combinations such as natural color, true color, and false color composite, etc. is used to identify the land use type in the study area (Kafy et al., 2020). During data processing, bands such as red, green, blue, and near-infrared bands were utilized for Landsat images to find true color in ERDAS Imagine 2014. The LULC type was classified into five classes (built-up area, vacant land, agricultural land, waterbodies, vegetation) by applying the MLC method (Bishta, 2018). To check the accuracy of LULC data, 130 training sites were randomly selected and calculated user, producer, and overall accuracy along with Kappa coefficient using equations 1-4. The overall accuracy was 95%, 87% and 93% for the three-study year with Kappa coefficient 0.957, 0.865, and 0.914 which implies the good accuracy of the image classification (Kafy et al., 2020).

$$User-accuracy = \frac{\text{Correctly classified pixel number in each category}}{\text{Total reference pixels in each category (row total)}} \times 100\% \quad (1)$$

$$Producer-accuracy = \frac{Num\ of\ correctly\ classified\ pixels}{Total\ numb\ of\ reference\ pixels\ in\ each\ category\ in\ column} \times 100\% \quad (2)$$

$$Overall-accuracy = \frac{\text{Total pixels classified correctly pixels}}{\text{Total reference pixels}} \times 100\% \quad (3)$$

$$Kappa-coefficient = \frac{Total\ sample\ num \times Total\ corrected\ sample\ num - \sum(col.tot \times row\ tot)}{Total\ sample\ num^2 - \sum col.tot \times row\ tot} \times 100\% \quad (4)$$

2.4. Land-specific carbon emissions (LCEs) estimation

The change in land use is well known as a net source of worldwide GHG emissions. Most of these emissions are due to losses from offshore pools such as deforestation (Ross et al., 2016). There are many carbon emissions sources. In this study, we focused on only land-specific carbon emissions sources. The LULC data were utilized to estimate the carbon emissions and absorption and their change pattern over the study period. In this regard, equation (5) is used (Cui et al., 2018).

$$LCEi = \sum Ai \times \delta i \times \left(\frac{MCO2}{MC}\right. \quad (5)$$

Where LCEi = CEs from i LULC type; i = LULC type; Ai = Area of I LULC type, δi = CE coefficient for i LULC type, $M_{CO2}/M_C = 44/12$.

The positive value of δi represents emissions and the negative figure specifies carbon absorption (Cui et al., 2018). Five LULC types were identified in this study through the MLC method while the value of CE coefficient for each LULC type in Table 2 has been proposed in the literature (Fang et al., 2007; Cui et al., 2018; Hong-xin et al., 2012) and Cui et al. (2018) validated these coefficients for South Asian region.

Table 2
The CE coefficient (δi) for the selected five LULC types.

LULC Type	CE coefficient ($kg(C)m^{-2}a^{-1}$)
Built-up	+0.0724
Waterbodies	−0.0459
Vacant land	−0.0005
Agricultural land	+0.0497
Vegetation	−0.0645

2.5. Derivation of LST

The land surface temperature of the study area was calculated for the year 1998, 2008 by using Landsat 5 TM, 2018 by Landsat 8 OLI satellite images. Landsat images encompass digital numbers (DNS). The following steps were followed to derive the LST (Gazi et al., 2020; Grigoraș and Uriț;escu, 2019).

$$L_v = A_v + (M_L \times Q_{CAL}) \quad (6)$$

L_v is the TOA spectral radiance in units $Wm^{-2}sr^{-1}\mu m^{-1}$; M_L indicates the radiance multiplicative scaling factor; A_v is the radiance additive scaling factor for the band; Q_{CAL} indicates the quantized calibrated pixel value in DNS.

In the next stage, the TOA spectral radiance (L_λ) values were converted to At-Satellite Brightness Temperature (TB)

$$TB = \frac{k_2}{\ln\left(\frac{k_1}{L_\lambda}\right) + 1} \quad (7)$$

Where for Landsat 8 OLI K_1 = 774.8853, K_2 = 1321.8883 and for Landsat 5 TM images K_1 = 607.76 and K_2 = 1260.56 are the thermal conversion constants for the band. The TB is converted to LST (in Kelvin) through equation (8).

$$LST = \frac{TB \times ln\ \varepsilon}{1 + \frac{\lambda \times TB}{\alpha}} \quad (8)$$

Where, λ = Emitted radiance's wave-length; α = hc/k = 1.438 × 10^{-2}mK; and ε indicates surface emissivity which calculated through equation (9).

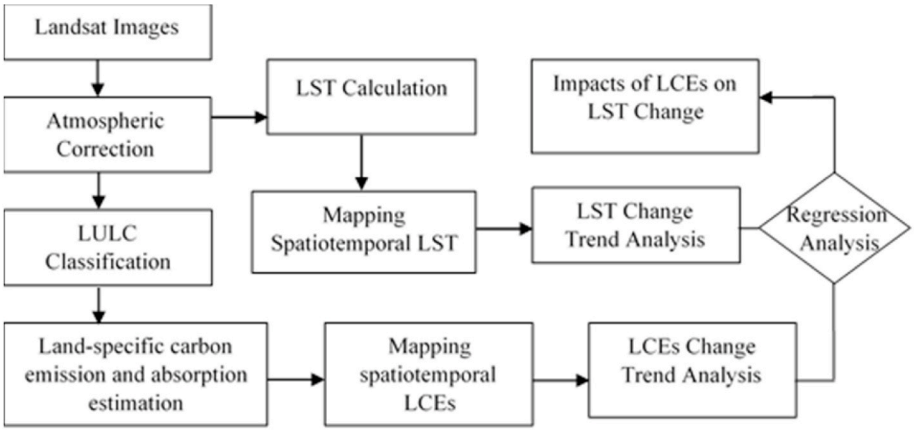

Fig. 2. Methodological flowchart of the study.

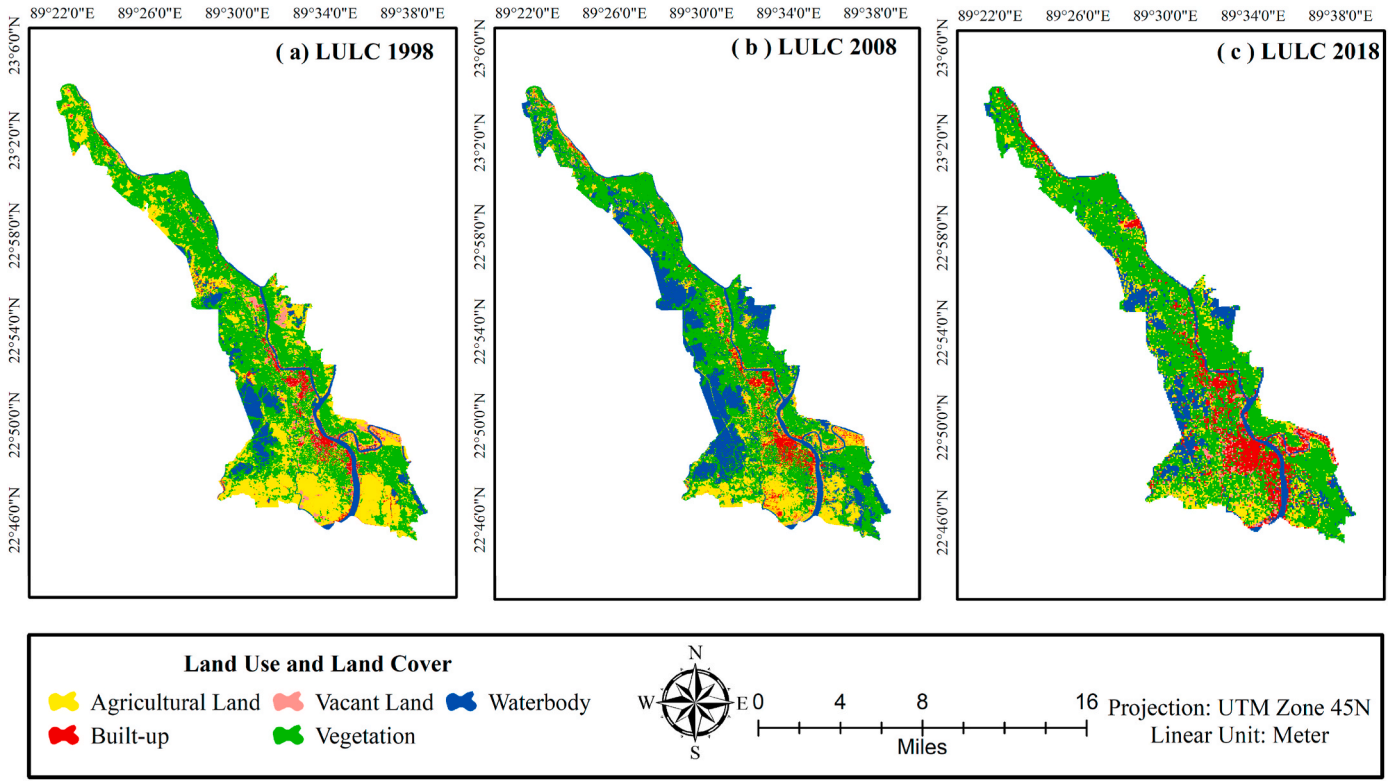

Fig. 3. LULC maps of the study area during 1998–2018.

Table 3
Derived LULC status in the study area during 1998–2018.

LULC	1998		2008		2018	
	Area (Km^2)	%	Area (Km^2)	%	Area (Km^2)	%
AL	72.17	30.89	41.35	17.69	28.94	12.39
BU	9.68	4.14	11.38	4.87	27.06	11.58
VL	7.94	3.40	5.93	2.54	7.99	3.42
VG	115.87	49.59	114.25	48.89	133.22	57.02
WB	28.00	11.98	60.76	26.01	36.45	15.60
Total	233.66	100%	233.66	100%	233.66	100%

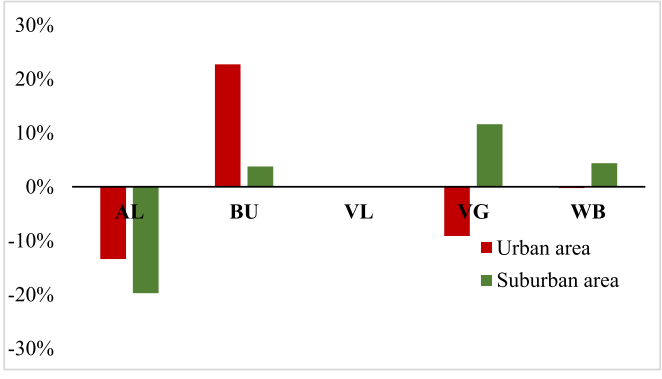

Fig. 4. LULC changes direction in urban and suburban areas.

$$\varepsilon = 0.004 \times Pv + 0.986 \tag{9}$$

$$Pv = \left[\frac{NDVI - NDVI\ min}{NDVI - NDVI\ max}\right]^2 \tag{10}$$

To get the LST in Celsius (°C) unit, 273.15 was subtracted from the initial LST values (K).

In Landsat 5 TM images, the thermal band (band 6) is used for the extraction of LST. The following equation (11) was utilized to derive the LST pattern from the Landsat 5 imageries (Grigoraș & Uriț;escu, 2019).

$$Lv = \frac{(LMax\lambda - LMinv) \times (QCAL - QCALMIN)}{QCALMAX - QCALMIN} + LMIN\lambda \tag{11}$$

Where, L_v is the TOA Spectral Radiance; L_{MAXv} is the spectral radiance that is scaled to $QCAL_{MAX}$ in units $Wm^{-2}sr^{-1}\mu m^{-}1$, $L_{MIN\lambda}$ is the spectral radiance that is scaled to $QCAL_{MIN}$; $QCAL_{MAX}$ indicates the maximum quantized calibrated pixel value and $QCAL_{MIN}$ is the minimum quantized calibrated pixel value.

2.6. Association between LCEs and LST

The association between LCEs and LST was determined by using the linear regression model in ArcGIS. In this regard, the spatiotemporal LCEs and LST data of different study periods were utilized. The response of LST to LCEs was also assessed for both urban and suburban areas through regression analysis. Fig. 2 represents the working procedure of the study followed to fulfill the objectives of the study.

3. Result and interpretation

3.1. LULC change analysis 1998–2018

The LULC status of the study area was obtained from Landsat images of the year 1998, 2008, and 2018 by applying the MLC method (Fig. 3).. Five LULC types have been identified and their status has been presented in Table 3. The vegetative areas covered about 115.87 Km^2 (49.59%) in 1998 and increased to 133.22 Km^2 (57.02%) in 2018. In urban areas, vegetative areas decreased by 9.41% (4.15 Km^2) and increased by 11.60% (21.14 Km^2) in the suburban area. The agricultural land was 30.89% (72.17 Km^2) in 1998 and decreased to 12.39% (28.94 Km^2) in

Table 4
Land-use based carbon emission and absorption statistics in the study area. (unit: × 1000 tons/year).

LULC	Urban area						Suburban area					
	1998		2008		2018		1998		2008		2018	
	LCE	%	LCE	%	LCE	%	LCE	%	LCE	%	LCE	%
AL	1.51	49.91	1.25	37.69	0.40	8.72	11.63	91.69	6.27	86.67	4.84	62.43
BU	1.52	50.19	2.06	62.17	4.25	93.24	1.05	8.28	0.96	13.29	2.91	37.51
VL	0.00	0.08	0.00	0.03	−0.01	0.09	−0.01	0.04	−0.01	0.03	−0.01	0.03
VG	−5.27	82.96	−4.96	77.24	−4.29	80.12	−22.11	85.88	−22.04	71.57	−27.10	84.44
WB	−1.08	17.01	−1.46	22.78	−1.06	19.82	−3.62	14.07	−8.74	28.40	−4.98	15.52
TE	3.02		3.31		4.65		12.68		7.24		7.75	
TA	−6.35		−6.42		−5.35		−25.74		−30.79		−32.10	
NE	−3.33		−3.12		−0.70		−13.06		−23.55		−24.35	

Here, LCE = Land-use based carbon emission, TE = Total emissions, TA = Total absorptions, NE= Net emission.

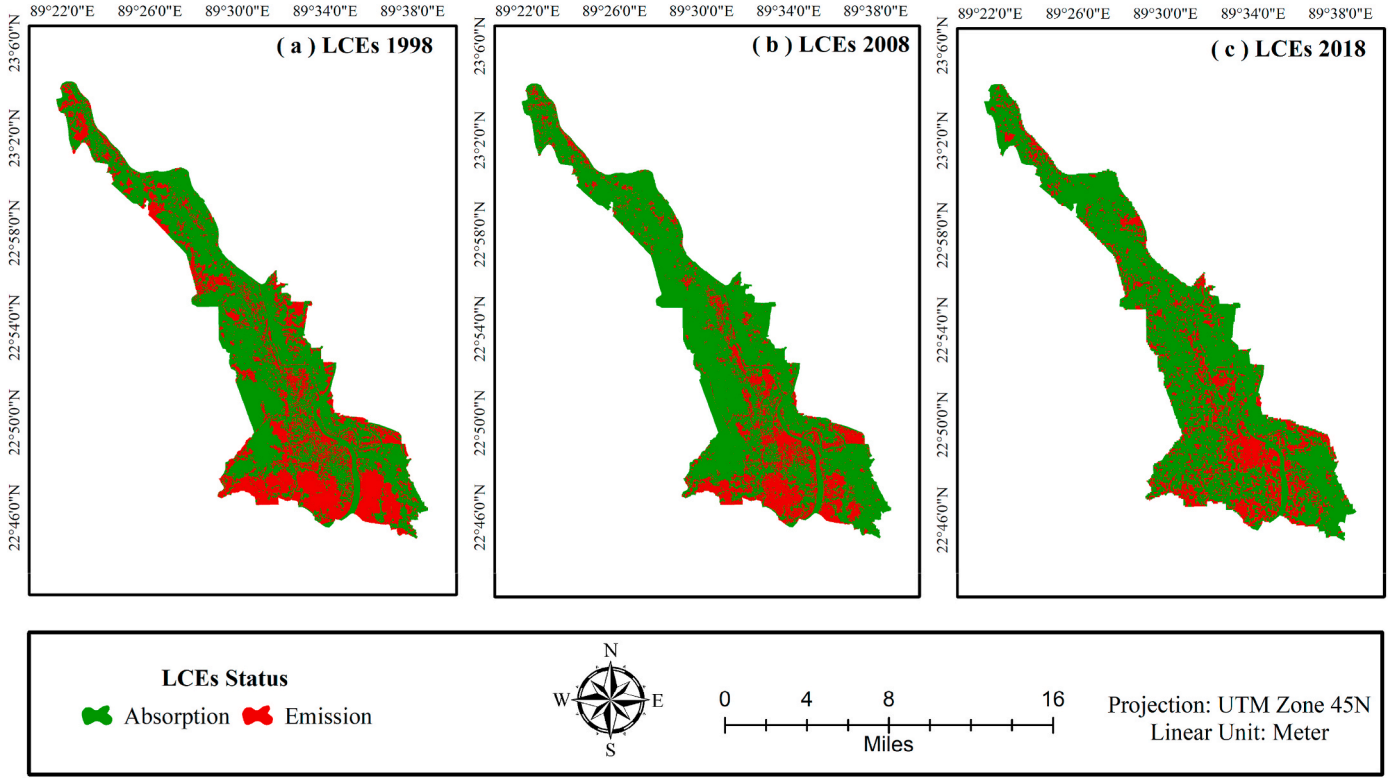

Fig. 5. Land-use based carbon emission and absorption map of the study area during 1998–2018.

2018. The analysis shows that about 43.23 Km^2 (18.50% of the total study area and 59.90% of agricultural land) agricultural land has lost during 1998–2018, due to the transformation of LULC types. In 1998, the waterbody area covered 28 Km^2 (11.98%), increased to 60.76 Km^2 (26.01%) in 2008 and declined to 36.45 Km^2 (15.60%) in 2018. In the suburban areas, agricultural areas decreased and transformed into built-up, vegetation, and waterbody area (Fig. 4). Due to urbanization and the increase of urban activities in the KCC area, the built-up area increased, and the natural landscape of the KCC area transformed into built-up areas (Fattah et al., 2021). The waterbody areas in the suburban area of Khulna are increased in the last few decades due to the increase in shrimp cultivation (Morshed et al., 2020a). According to Morshed et al. (2020b) due to the soil salinity and its inclination, crop production in Khulna is becoming unsuitable, and an increase in shrimp exports attracted farmers in shrimp-cultivation that triggered waterbody areas.

The percentage of built-up areas in both urban and suburban areas is increasing at a noticeable rate to fulfill the growing needs of the residents. The built-up areas were increased from 9.68 Km^2 (4.14%) to 27.06 Km^2 (11.58%) during 1998–2018 whereas, the built-up area increased by 10.31 Km^2 in urban and by 7 Km^2 in suburban areas. This increasing rate of built-up areas depicts that the declination of eco-friendly LULC is pushing the environment of the study area towards imbalance and anomalous LCEs.

3.2. Carbon emission pattern

By using the LULC data in Table 3, derived from the MLC process, land-use-based carbon emissions and absorptions were estimated for the year 1998, 2008, and 2018 with equation (5) (Table 4) and represented in the map in Fig. 5. Negative figures indicate carbon sinks such as vacant land, waterbodies, and vegetation areas while the positive figures for the built-up area and agricultural lands refer to carbon emission sources (Table 4). The vegetation and built-up area were the largest contributors to carbon absorptions and emissions respectively in the urban areas while agricultural land is the largest emission source of suburban areas. The total emissions were found to decrease from 15698.63 to 12394.52tons/year and total absorption increased from 32089.88 to 37447.10tons/year. The increased amount of carbon sinks

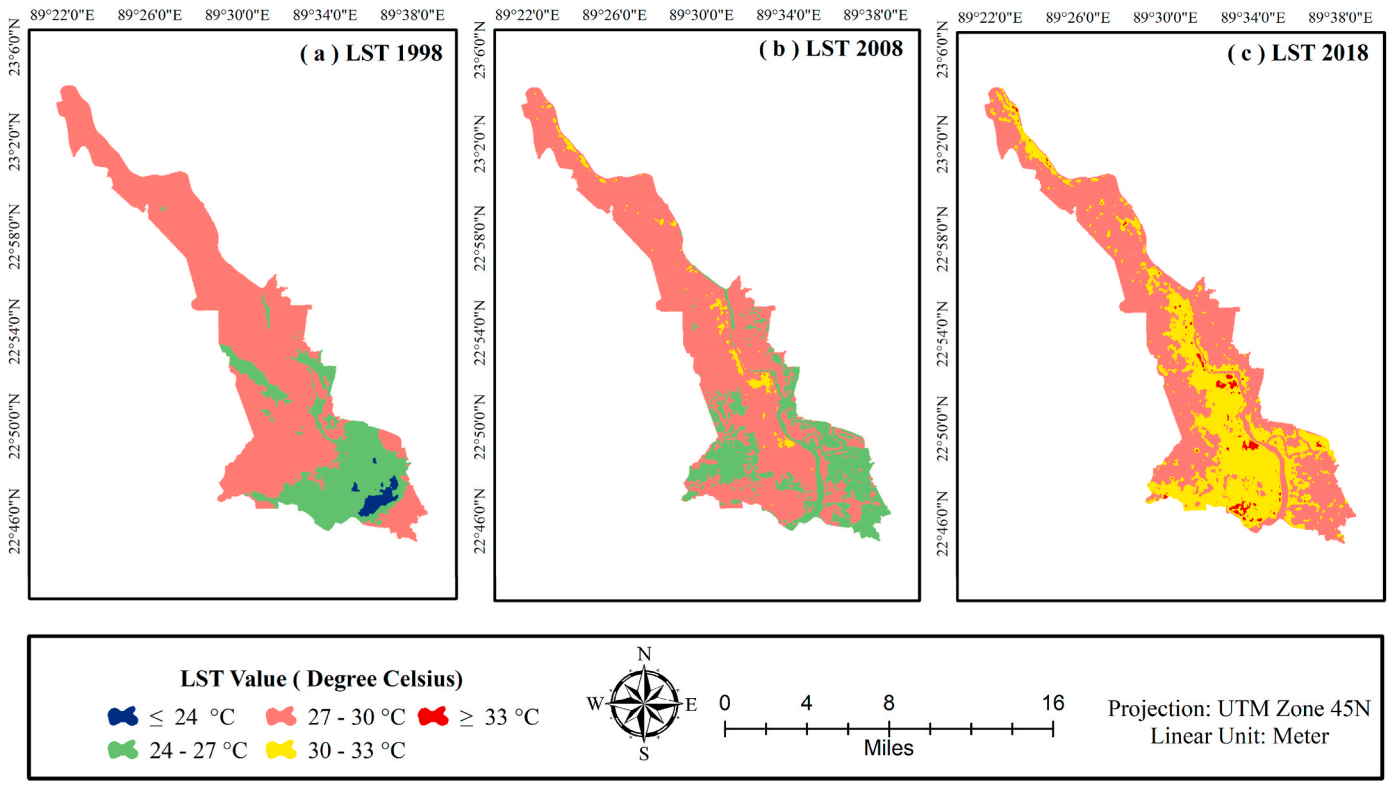

Fig. 6. LST map of the study unit during 1998–2018.

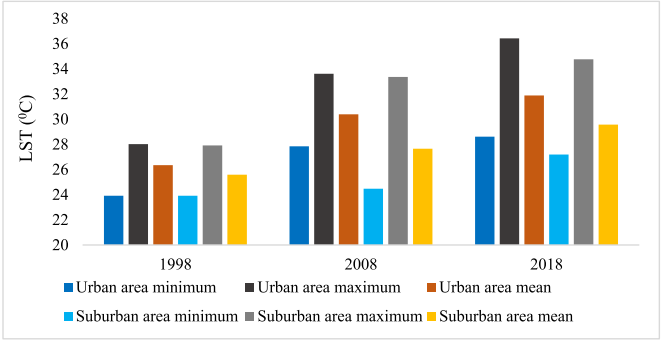

Fig. 7. Mean, minimum, and maximum LST distribution in the urban and suburban areas.

Table 5
Distribution of LST in classified temperature ranges.

LST range (^{0}C)	1998		2008		2018	
	Area (Km^2)	%	Area (Km^2)	%	Area (Km^2)	%
≤ 24	4.01	1.72	0.00	0.00	0.00	0.00
24–27	58.19	24.90	59.63	25.52	0.00	0.00
27–30	171.46	73.38	167.80	71.80	143.68	61.49
30–33	0.00	0.00	6.22	2.66	86.42	36.98
≥ 33	0.00	0.00	0.03	0.01	3.54	1.53
Total	233.66	100%	233.66	100%	233.66	100%

such as vegetation and waterbody have triggered the carbon absorptions and have reduced the total emissions during the study period.

Table 4 shows that the LCEs change pattern during 1998–2018 in urban and suburban areas is opposite. The total emission in the urban area increased from 3022.87 to 4693.38tons due to the increase of built-up areas and declination of waterbody and vegetation LULC area reduced the total absorption from 6352.71 to 5351.87tons in the urban area. As a result, net emissions increased by 2627.30tons in the urban area with a rate of 1313.65tons/decade. While the transformation of agricultural land into waterbody and vegetation area reduced total CEs from 12675.65 to 7745.18tons and increased absorptions capacity from 25737.17 to 320952.54tons/year during the study period in suburban area. Due to the different LULC change patterns in the urban and sub-urban areas of the study area, the LCEs change pattern has also been observed differently. In urban area 4.76 Km^2 (10.48% of urban area) carbon sinks transformed into carbon sources while 30.26 Km^2 (16.10% of the suburban area) carbon sources transformed into carbon sinks. This LCEs increasing trend in the urban area will lead to environmental degradation.

Table 6
The atmospheric condition in the respected month of Landsat image acquisition (Source http://climate.barcapps.gov.bd/dashboard).

Weather	1998	2008	2018
Temp. Min (^{0}C)	23.45	23.87	23.16
Temp. Max (^{0}C)	33.65	34.97	34.34
Rainfall (mm)	105.00	36.00	64.00
Humidity	77.20%	74.79%	73.83%

3.3. LST change analysis

The LST range was confined between 23.91°C–28.02°C in 1998, 24.48°C–33.61°C in 2008 and 27.18°C– 36.42°C in 2018 (Fig. 6). The highest LST was observed in the KCC area which is the urban area. The mean, minimum, and maximum LST of both urban and suburban areas during the study years are presented in Fig. 7. Table 5 shows that a total of 171.46 Km^2 (73.38%) area represents the LST from 27^{0}C–30 °C followed by 58.19 Km^2 (24.90%) area faced 24^{0}C–27 °C and 4.01 Km^2 (1.72%) area faced LST ≤ 24 °C in 1998. The highest LST 28.02 °C was

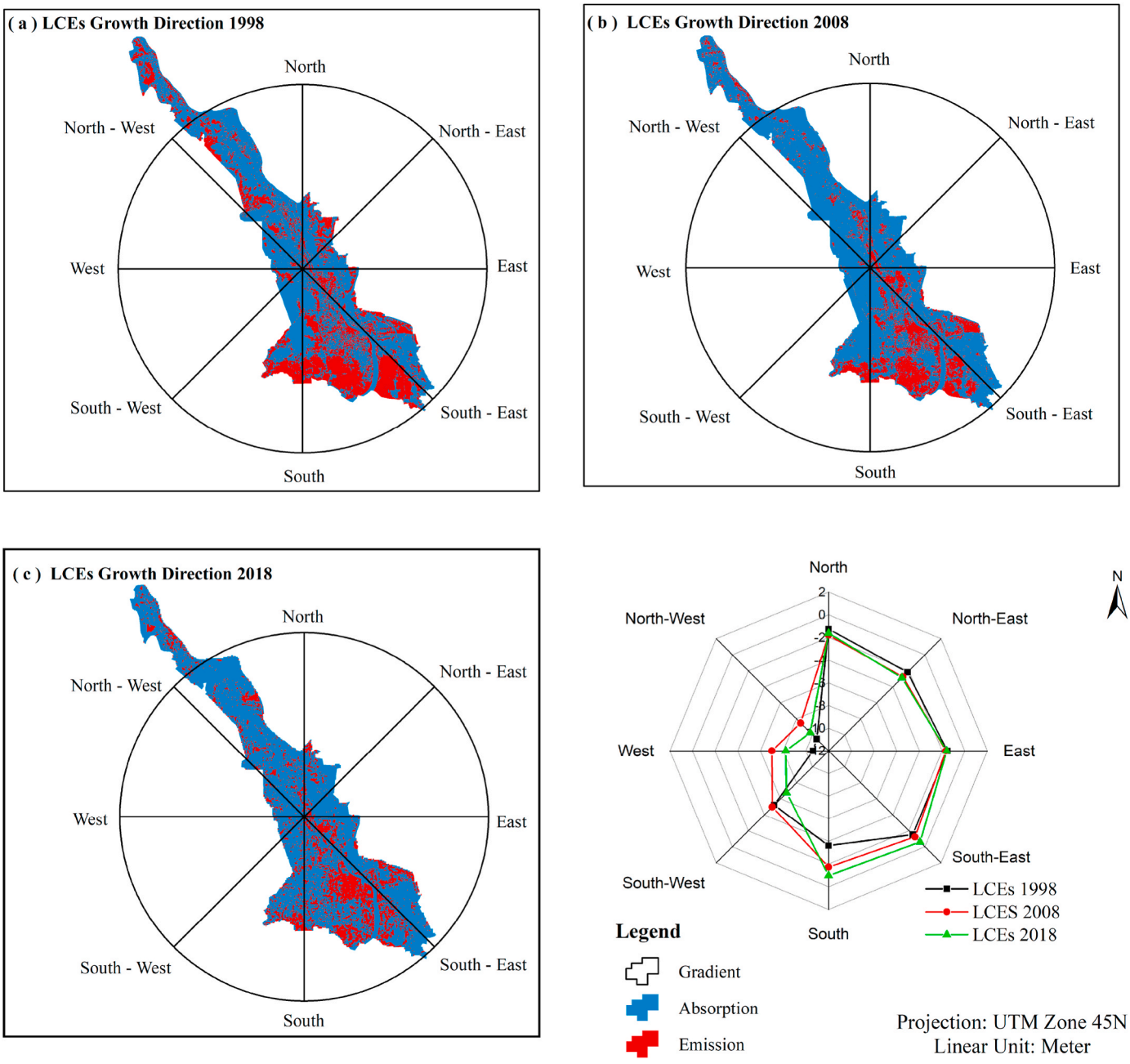

Fig. 8. Gradient map showing the LCEs change direction during 1998–2018 (Unit: LCEs in × 10^3 tons/year; LST in × 10 °C).

observed in KCC and the lowest LST 23.91 °C in the suburban area. In 2008, 2.66% (6.22 Km^2) of the total study areas had LST between 30^0C–33 °C and in 2018 this percentage increased to 36.98% (86.42 Km^2). Only 0.01% areas LST was ≥33 °C in 2008 which also increased to 1.53% (3.54 Km^2) in 2018. In 2018, the mean LST observed 31.89 °C in urban areas and 29.73 °C in suburban areas. The percentage of area under different LST range suggests that the surface temperature of Khulna was increased dramatically and the mean LST increased by 5.54 °C in the urban area and 4.14 °C in the suburban areas during the study period. The atmospheric weather data of Khulna collected from BMD to verify LST in the respected year and month of Landsat image acquisition (Table 6**)** which shows the average atmospheric condition and no sign of drought. The analysis demonstrated the increase of mean, minimum, and maximum temperature including atmospheric temperature with the increase of carbon emissions sources. A relatively higher temperature has been observed in the urban area (Fig. 7) and whereas the carbon sinks (waterbody and vegetation LULC) mostly showing lower LST.

3.4. Association between LCEs and LST

The change analysis of LCEs and LST showed the increasing trend of both LST and LCEs during the study period. The LST found comparatively lower in the carbon sinks and higher in the carbon sources. Surface temperatures showed an increasing trend with the increase of carbon emission (Fig. 10). To understand the LCEs and LST change better, a direction-based analysis is much better and Fig. 8 represents the LCEs increase scenario and Fig. 9 LST increase direction scenario of the study area. During 1998, the lowest temperature observed 23.91 °C in carbon sink areas with LCEs value −28240 tons/year and 28.02 °C at carbon sources having LCEs value 4000.07 tons/year. During 1998–2018, CEs in the urban area has been increased as a result LST

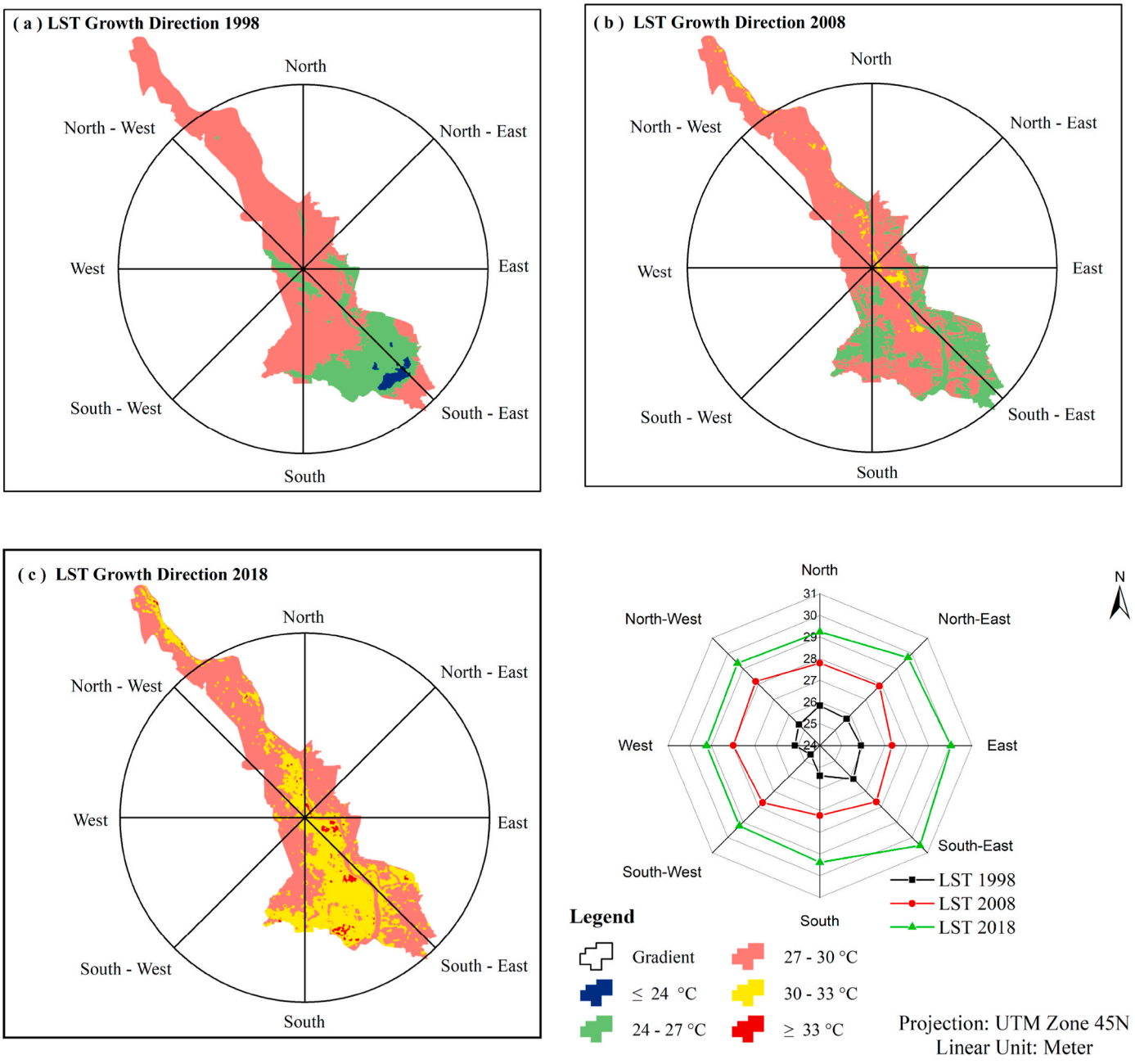

Fig. 9. Gradient map showing the LST change direction during 1998–2018.

increased to maximum 36.42 °C. Due to the increase of carbon absorption sources in the suburban areas, the LST growth was relatively lower in suburban areas than in urban areas. The gradient graph in Fig. 8 and statistics in Table 7 shows that LST increased in the same direction where the LCEs have increased. In 1998, lowermost LST was 24.60 °C in southwest direction where the LCEs was -5.23×10^3tons/year, maximum LST was observed 26.18 °C in southeast direction and LCEs was -1.52×10^3tons/year. In 2018, lowermost LST was 29.24 °C in the southwest direction with LCEs value -6.77×10^3tons/year while higher-most LST 30.52 °C in the southeast direction with LCEs values -0.60×10^3tons/year.

The outcome of the regression analysis between carbon emission and LST for different years is presented in Fig. 10a-c. Section 3.2 and 3.3 show the variation in the LCEs and LST change patterns in urban and suburban areas. In this regard, correlation coefficients (R^2) were also calculated for the regression analysis between LCEs and LST values for both urban and suburban areas Fig. 10d-i. The R^2 values are positive and become higher from 1998 to 2018. For the whole study area, the R^2 values were calculated 0.82651, 0.83751, and 0.89216 for the respective year which implies a strong positive correlation between LCEs and LST. Having a positive and strong correlation indicates that the more carbon emits the higher the surface temperature.

The R^2 value of urban and suburban area in 1998 were 0.80151 and 0.77741 (Fig. 10d, g); 0.8913 and 0.84774 in 2008 (Fig. 10e, h), 0.89562 and 0.75962 in 2018 (Fig. 10f, i). These R^2 indicates that the LST responded highly to the increase of LCEs in the urban areas than in the suburban areas. LST increased rapidly in the urban area as CEs and carbon emission sources have increased in urban areas. On the other hand, due to the increase in carbon sink areas and absorption capacity in the suburban area, the increase of LST and response have been relatively low. The regression analysis reveals that the increase of LCEs contributed significantly to the rise of LST in the study area during the study

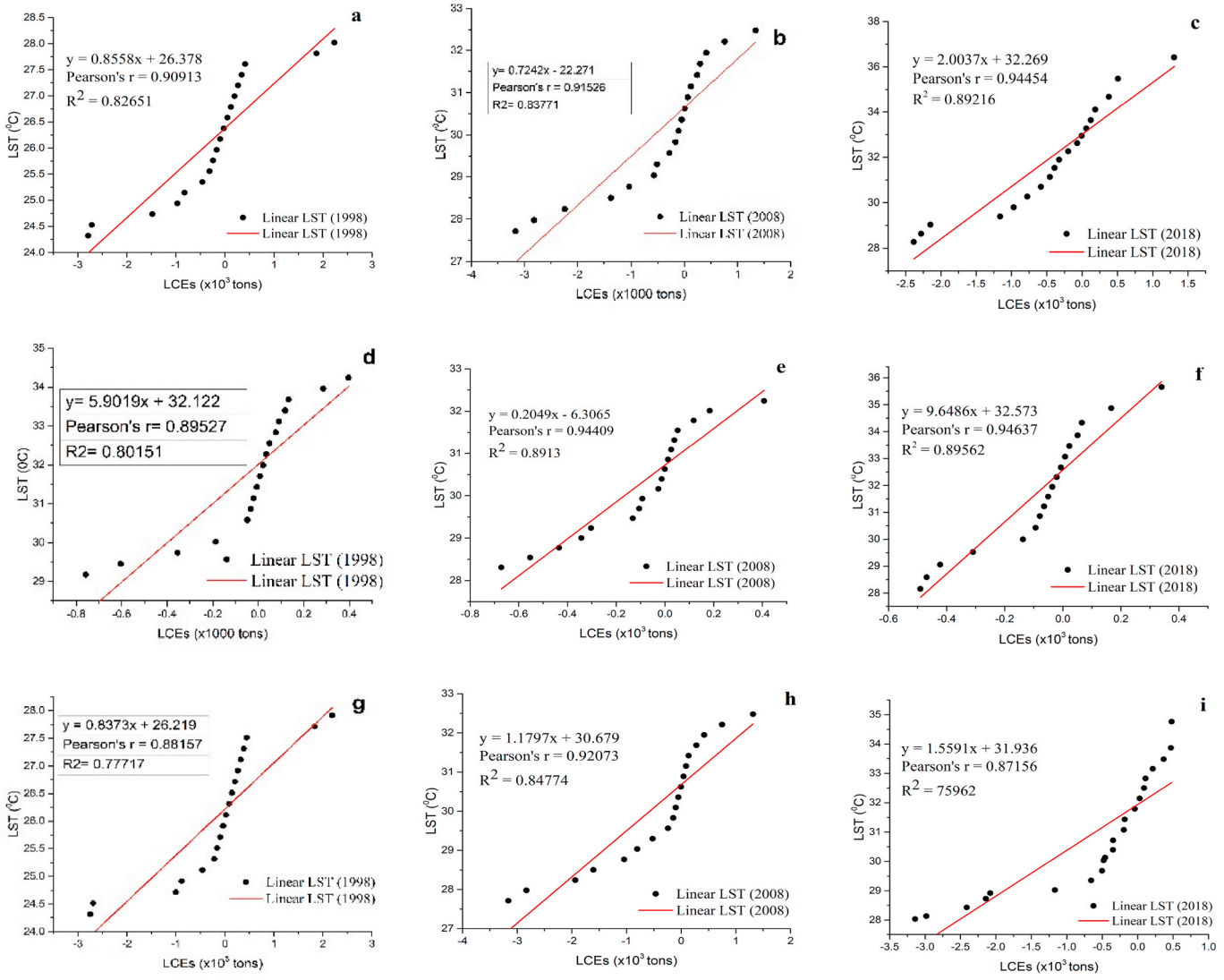

Fig. 10. Correlation between LCEs and LST for KDA area in (a) 1998 (b) 2008 (c) 2018; for urban area in (d) 1998 (e) 2008 (f) 2018; and for suburban area (g) 1998 (h) 2008 (i) 2018.

Table 7
LCEs and LST growth direction statistics. (Unit: LST in ^{o}C, LCEs in $\times$ 10^{3}tons/year).

Direction	1998		2008		2018	
	LCEs	LST	LCEs	LST	LCEs	LST
South-West	−5.23	24.60	−4.99	27.73	−6.77	29.24
South	−3.62	25.38	−1.73	27.23	−0.98	29.39
South-East	−1.52	26.18	−1.25	27.67	−0.61	30.52
East	−1.54	25.89	−1.66	27.31	−1.59	30.03
West	−10.62	25.15	−7.01	27.99	−8.22	29.22
North-East	−2.18	25.74	−2.75	27.88	−2.87	29.73
North-West	−10.53	25.36	−8.52	28.18	−9.71	29.36
North	−1.26	25.84	−1.79	27.80	−1.61	29.24

period.

4. Discussion

Urbanization in all the countries is common, while their growth patterns vary due to different urban planning and administrative policies also for different landscapes (Gazi et al., 2020). Although urban development can encourage developmental improvements that improve the living conditions of people, it can lead to increasingly severe thermal effects as well. Urban expansion is gradually affecting the environment of the city as well as the suburban area. This study found that the agricultural lands of the urban and suburban areas of Khulna have gone through rapid LULC transformation. In urban areas, about 17.38Km2 built-up area has been increased which increased LCEs from 3.02 $\times$ 10^{3} to 4.65 $\times$ 10^{3} tons/year during 1998–2018 while increased carbon sinks have increased the carbon absorption capacity of suburban area by 6.36 $\times$ 10^{3} tons/year. As a result, the LST value ranges increased from 23.91 °C–28.02 °C–24.48 °C–33.61 °C during 1998–2008 and increased to 27.18 °C–36.42 °C in 2018. The increase of LCEs and reduction of carbon absorption capacity of the urban land cover increased LST of the urban areas by 5.54 °C with a rate of 0.277 °C/year while reduction of LCEs in the suburban area has reduced the growth rate to 0.207 °C/year. The minimum, maximum and mean LST of the urban area recorded higher in the urban area than in the suburban area due to higher LCEs. The minimum LST in carbon sinks and highest LST in the carbon sources in all the three-study years imply that the higher the LCEs, the higher the LST.

The gradient map shows that the increase in LCEs influences the rise of LST in the same direction. The correlation coefficient 0.82651, 0.83771, and 0.89216 of regression analysis between LCEs and LST of

the consecutive year indicates the strong positive influence of LCEs on the rise of LST in the study area. The higher R^2 values of the urban area (0.80151, 0.8913, 0.89562) than of the suburban area (0.77717, 0.84774, 0.75962) indicate that the surface temperature of the urban area motivated highly by the LCEs pattern of the urban area. The findings of the study concluded that higher LCEs increase the rate of surface temperature growth and by increasing the carbon sink areas, it is possible to reduce the higher LST growth rate. The overall study signifies the need for proper implementation of planning rules and regulations to reduce the LCEs, otherwise surface temperature will accelerate enormously, and soon the Khulna will transform into an uninhabitable city.

5. Conclusion

Rapid urbanization with extensive economic activities resulted in rapid urban expansion, destruction of eco-friendly land cover, increase of GHG emission, global warming, etc., and making the living environment more unhabitable gradually. Due to unplanned urbanization, the cities of developing countries are facing severe adverse environmental changes. The surface temperature, as well as atmospheric temperature in the cities of Bangladesh, has been increasing rapidly. The result of this study reveals the increasing LCEs pattern in the urban areas of Bangladesh triggering the surface temperature with a higher LST change rate. The destruction of carbon sinks and the increase of carbon sources intensified the LST of the study area. The positive coefficient indicates that the increase LST becomes stronger as the LCEs increase and LCEs change pattern have a strong influence on the LST change pattern. There may be other reasons for the LST rise, but our results suggest that the increase of LCEs is a significant cause. When the carbon emission sources increase, the carbon absorption capacity of the area decreases and contributes to surface warming. This outcome highlights the fact that the transformation of carbon sink areas into carbon emission sources has a significant influence on local climate, and the increase of ecofriendly land cover decreases the surface temperature by absorbing carbon from the environment. This study provides a scientific reference for urban-managers, urban-planners, and policymakers working towards a healthy and sustainable Khulna city.

Funding

There was no funding for this research.

Author's statement

All persons who meet authorship criteria are listed as authors, and all authors certify that they have contributed equally.

Declaration of competing interest

The authors declare that they have no known competing financial interests or personal relationships that could have appeared to influence the work reported in this paper.

Appendix A. Supplementary data

Supplementary data to this article can be found online at https://doi.org/10.1016/j.rsase.2021.100508.

References

Ahmed, B., 2011. Modelling spatio-temporal urban land cover growth dynamics using remote sensing and GIS techniques: a case study of Khulna City. J. Bangladesh Inst. Plan. 4, 15–32.

Ahmed, B., Kamruzzaman, M.D., Zhu, X., Shahinoor Rahman, M.D., Choi, K., 2013. Simulating land cover changes and their impacts on land surface temperature in Dhaka, Bangladesh. Rem. Sens. 5, 5969–5998.

Alawamy Suliman, Jamal, Balasundram, Siva K., Mohd, Ahmad Husni, Sung, Christopher Teh Boon, 2020. Detecting and Analyzing Land Use and Land Cover Changes in the Region of Al-Jabal Al-Akhdar, Libya Using Time-Series Landsat Data from 1985 to 2017. Sustainability 12 (11), 4490. https://doi.org/10.3390/su12114490.

Baccini, A., Goetz, S.J., Walker, W.S., Laporte, N.T., Sun, M., Sulla-Menashe, D., Houghton, R.A., 2012. Estimated carbon dioxide emissions from tropical deforestation improved by carbon-density maps. Nat. Clim. Change 2, 182–185.

BBS, 2011. Population and housing census (2011). Bangladesh Bureau of Statistics (BBS). Ministry of Planning, Government of the People's Republic of Bangladesh, Dhaka.

Bishta, A.Z., 2018. Assessment of the reliability of supervised classifications of Landsat-7, ASTER, and SPOT-5 multispectral data in rock unit discriminations of Jabal Daf-Wadi Fatima area, Saudi Arabia. Arabian Journal of Geosciences 11.

Chuai, Xiaowei, Huang, Xianjin, Wang, Wanjing, Wu, Changyan, Zhao, Rongqin, 2014. Spatial Simulation of Land Use based on Terrestrial Ecosystem Carbon Storage in Coastal Jiangsu, China. SCIENTIFIC REPORTS 4, 5667. https://doi.org/10.1038/srep05667.

Cui, Y., Li, L., Chen, L., Zhang, Y., Cheng, L., Zhou, X., Yang, X., 2018. Land-use carbon emissions estimation for the yangtze river delta urban agglomeration using 1994-2016 Landsat image data. Rem. Sens. 10.

Don, A., Schumacher, J., Freibauer, A., 2011. Impact of tropical land-use change on soil organic carbon stocks - a meta-analysis. Global Change Biol. 17, 1658–1670.

Duguma, L., Atela, J., Minang, P., Ayana, A., Gizachew, B., Nzyoka, J., Bernard, F., 2019. Deforestation and forest degradation as an environmental behavior: unpacking realities shaping community actions. Land 8, 26.

Fang, J., Guo, Z., Piao, S., Chen, A., 2007. Terrestrial vegetation carbon sinks in China, 1981–2000. Sci. China Earth Sci. 50, 1341–1350.

Fang, J.Y., Zhu, J.L., Wang, S.P., Yue, C., Shen, H.H., 2011. Global warming, human-induced carbon emissions, and their uncertainties. Sci. China Earth Sci. 54, 1458–1468.

Fattah, M., Morshed, S.R., Morshed, S.Y., 2021. Multi-layer perceptron-Markov chain-based artificial neural network for modelling future land-specific carbon emission pattern and its influences on surface temperature. SN Appl. Sci. 3, 359. https://doi.org/10.1007/s42452-021-04351-8.

Florides, G.A., Christodoulides, P., 2009. Global warming and carbon dioxide through sciences. Environ. Int. 35, 390–401.

Friedlingstein, P., Houghton, R.A., Marland, G., Hackler, J., Boden, T.A., Conway, T.A., Quéré, C., 2010. Update on CO2 emissions. Nat. Geosci. 3, 811–812.

Gazi, M.Y., Rahman, M.Z., Uddin, M.M., et al., 2020. Spatio-temporal dynamic land cover changes and their impacts on the urban thermal environment in the Chittagong metropolitan area, Bangladesh. GeoJournal. https://doi.org/10.1007/s10708-020-10178-4.

Grigoraș, G., Urițescu, B., 2019. Land use/land cover changes dynamics and their effects on surface urban heat island in bucharest, Romania. Int. J. Appl. Earth Obs. Geoinf. 80, 115–126.

Guha, S., Govil, H., Dey, A., Gill, N., 2018. Analytical study of land surface temperature with NDVI and NDBI using Landsat 8 OLI and TIRS data in Florence and Naples city, Italy. European Journal of Remote Sensing 51, 667–678.

Haque, A.N., Dodman, D., Hossain, M.M., 2014. Individual, communal and institutional responses to climate change by low-income households in Khulna, Bangladesh. Environ. Urbanization 26 (1), 112–129. https://doi.org/10.1177/0956247813518681.

Hong-xin, S., Xing-min, M., Ying-long, Z., Ming-quan, L., 2012. Effects of different land use patterns on carbon emission in guangyuan city of sichuan province. Bull. Soil Water Conserv. 32, 101–106.

Houghton, R.A., House, J.I., Pongratz, J., Van Der Werf, G.R., Defries, R.S., Hansen, M.C., Le Quéré, C., Ramankutty, N., 2012. Carbon emissions from land use and land-cover change. Biogeosciences 9, 5125–5142.

Islam, S., Ma, M., 2018. Geospatial monitoring of land surface temperature effects on vegetation dynamics in the southeastern region of Bangladesh from 2001 to 2016. ISPRS Int. J. Geo-Inf. 7.

Jain, N., Bhatia, A., Pathak, S., Gupta, N., Sharma, D., Kaushik, R., 2015. Greenhouse gas emission and global warming. In: Khoiyangbam, R.S., Gupta, N. (Eds.), Introduction to Environmental Sciences. TERI Press, India, pp. 379–411.

Jeevalakshmi, D., Narayana Reddy, S., Manikiam, B., 2017. Land surface temperature retrieval from LANDSAT data using emissivity estimation. Int. J. Appl. Eng. Res. 12, 9679–9687.

Kafy, A.-A., Abdullah-Al- Faisal, Sikdar, S., Hasan, M.M., Rahman, M., Khan, M.H., Islam, R., 2019. Impact of LULC changes on LST in rajshahi district of Bangladesh: a remote sensing approach. Journal of Geographical Studies 3, 11–23.

Kafy, A.A., Al-Faisal, A., Mahmudul Hasan, M., Sikdar, M.S., Hasan Khan, M.H., Rahman, M., Islam, R., 2020. Impact of LULC changes on LST in rajshahi district of Bangladesh: a remote sensing approach. Journal of Geographical Studies 3, 11–23.

Lai, L., Huang, X., Yang, H., Chuai, X., Zhang, M., Zhong, T., Chen, Z., Chen, Y., Wang, X., Thompson, J.R., 2016. Carbon emissions from land-use change and management in China between 1990 and 2010. Sci. Adv. 2, 1–8.

Li, C., Wang, J., Wang, L., Hu, L., Gong, P., 2014. Comparison of classification algorithms and training sample sizes in urban land classification with Landsat thematic mapper imagery. Rem. Sens. 6, 964–983. https://doi.org/10.3390/rs6020964.

Lin, X., Xu, M., Cao, C., Singh, R.P., Chen, W., Ju, H., 2018. Land-use/land-cover changes and their influence on the ecosystem in Chengdu City, China during the period of 1992-2018. Sustainability 10, 1–20.

Maheshwari, H., Chandra, U., Jain, K., 2018. A Review from Greenhouse Effect to Carbon Footprint. May 2019.

Maksudurrahman, M., 2018. Monitoring landuse/land cover change and its subsequent effects on urban thermal environment in Chittagong metropolitan area: a remote sensing and GIS based analysis kaniz farzana * 1, 59, 51–68.

Minnen, J.G., Goldewijk, K.K., Stehfest, E., Eickhout, B., Drecht, G.V., Leemans, R., 2009. The importance of three centuries of land-use change for the global and regional terrestrial carbon cycle. Climatic Change 97, 123.
Mohajan, H.K., 2014. Greenhouse gas emissions of China. Journal of Environmental Treatment Techniques 1, 190–202.
Mondal, K.K., Akhter, M.A., Mallik, M., Hassan, S., 2017. Study on rainfall and temperature trend of Khulna division in Bangladesh. DEW-DROP 4.
Morshed, M.M., et al., 2020a. Application of remote sensing for salinity based coastal land use zoning in Bangladesh. Spat. Inf. Res. https://doi.org/10.1007/s41324-020-00357-3.
Morshed, M.M., et al., 2020b. Production externalities of shrimp aquaculture on paddy farming in coastal Bangladesh. Agric. Water Manag. 238, 106213. https://doi.org/10.1016/j.agwat.2020.106213.
Ning, J., Gao, Z., Meng, R., Xu, F., Gao, M., 2018. Analysis of relationships between land surface temperature and land use changes in the Yellow River Delta. Front. Earth Sci. 12, 444–456.
Parvin, N.S., Abudu, D., 2017. Estimating urban heat island intensity using remote sensing techniques in Dhaka city. Int. J. Sci. Eng. Res. 8, 289–298.
Peng, W., Zhou, J., Wen, L., Xue, S., Dong, L., 2017. Land surface temperature and its impact factors in Western Sichuan Plateau, China. Geocarto Int. 32, 919–934.
Prabha, A.C.S., Senthivelu, M., Paramasivam, A., 2019. Carbon sequestration potential in different land uses: a review. Int. J. Environ. Res. Dev. 15 (9), 727–736.
Quéré, C.L., Raupach, M.R., Canadell, J.G., Marland, G., Bopp, L., Ciais, P., Gurney, K., 2009. Trends in the sources and sinks of carbon dioxide. Nat. Geosci. 2, 831–836.
Ross, et al., 2016. Land use, land use change and soil carbon sequestration in the St. Johns River Basin, Florida, USA. Geoderma Regional 7 (19–28).
Raja, D.R., Neema, M.N., 2013. Impact of urban development and vegetation on land surface temperature of Dhaka city. In: International Conference on Computational Science and its Applications, vol. 7. Springer, Berlin, Heidelberg, pp. 351–367.
Sahana, M., Ahmed, R., Sajjad, H., 2016. Analyzing land surface temperature distribution in response to land use/land cover change using split window algorithm and spectral radiance model in Sundarban Biosphere Reserve, India. Modeling Earth Systems and Environment 2, 1–11.
Stern, N., 2014. The Economics of Climate Change: the Stern Review. Cambridge University Press, Cambridge, United Kingdom.
Zullo, F., Fazio, G., Romano, B., Marucci, A., Fiorini, L., 2019. Effects of urban growth spatial pattern (UGSP) on the land surface temperature (LST): a study in the Po Valley (Italy). Sci. Total Environ. 650, 1740–1751.